Superballistic characteristics in transient phonon ballistic-diffusive transport

Dao-Sheng Tang (唐道胜) and Bing-Yang Cao (曹炳阳)[a)]
Key Laboratory of Thermal Science and Power Engineering of Ministry of Education, Department of Engineering Mechanics, Tsinghua University, Beijing 100084, People's Republic of China

(Received 12 May 2017; accepted 3 September 2017; published online 15 September 2017)

While diffusive, superdiffusive, and ballistic phonon transports have been widely investigated, the superballistic phenomenon, where the time index of the energy mean square displacement with respect to time is greater than 2, has been neither predicted nor observed. In this work, we report on the superballistic characteristics obtained from simulations of transient phonon ballistic-diffusive transport both during and after the input of a heat pulse into a nanoscale film. The superballistic behaviors are well described by a previously proposed model for electron wave packet spreading employing a point source and further explained by the superposition effect of heat pulses. The relative superposition time, a dimensionless parameter, is defined to describe the degree of the heat pulse superposition. The analysis of superballistic characteristics in this work is expected to guide experiments for detecting the phonon superballistic transport. Also, it provides a potential phenomenological description for the superballistic phenomena in more complex systems. *Published by AIP Publishing*. [http://dx.doi.org/10.1063/1.5003639]

Transport phenomena, such as phonon transport and electron transport, can be divided into different regimes according to the energy mean square displacement (MSD)-time relationships based on the Brownian motion theory.[1–11] The energy MSD is defined as[3,4]

$$\langle \sigma^2(t) \rangle = \frac{\int_0^X (E(x,t) - E_0)(x - x_0)^2 dx}{\int_0^X (E(x,t) - E_0) dx} \sim t^\beta, \qquad (1)$$

where $\langle . \rangle$ represents an ensemble average, X is the maximum propagation distance, $E(x,t)$ is the total energy at position x and time t during the propagation process, E_0 is the background energy, x_0 is an initial position, and β is the time index. Generally, the energy MSD is a power function of time, and the value of β differs for different transport regimes. Diffusive transport ($\beta = 1$), which is regarded as the general form of transport, has been widely investigated.[12] Subdiffusive transport ($\beta < 1$),[13–18] superdiffusive transport ($1 < \beta < 2$),[3–5,19–23] and ballistic transport ($\beta = 2$)[24–28] have also been observed and discussed under both classical[3–5] and quantum conditions.[6–11] It was generally accepted that $\beta \leq 2$ for all types of transport until Hufnagel *et al.*[8,9] proposed the superballistic ($\beta > 2$) spreading of the electron wave packet, in particular, quantum systems. Recently, the superballistic transport of the optical wave packet in hybrid ordered-disordered photonic lattices was also experimentally studied.[29] However, superballistic transport has not been defined strictly. It is often explained as conditions where a particle moves faster during the transport process, as reflected by the MSD-time relationships.[6–11] Several descriptions have been proposed for superballistic transport, which generally contain fractional kinetic equations,[30] asymptotical solutions of the continuum-time random walk,[31] and generalized Langevin equations.[32] Siegle *et al.*[33] investigated hyperdiffusion phenomena originating from long-range velocity correlations by means of a generalized Langevin equation, based upon which the authors proposed a model of the force field and the initial thermal bath. Generally, force field models for non-diffusive transport are complicated and nonlinear and involve time dependencies, resulting in a non-Markovian process. Zhang *et al.*[9] studied non-diffusive electron packet spreading in several different types of quantum system lattices, including quasi-periodic lattices, disordered lattices, ordinary lattices, and combinations thereof. Actually, superballistic transport can occur for different kinds of quantum excitations besides electrons. Zimbardo *et al.* analyzed the ion superballistic transport in tearing driven magnetic turbulence.[6] Iubini *et al.* investigated the exciton transport coupled to an underlying spatially extended nonlinear chain of atoms and found that the propagation is faster than ballistic at the very first stage when the exciton-phonon coupling strengths are large.[34]

While past studies have considered superballistic phenomena, these phenomena have been neither predicted nor discussed for phonon transport. Phonon transport is not commonly influenced by external fields but by phonon-phonon scatterings. Anomalous physical phenomena and mechanisms related to various transport regimes may take place. In ultrafast/nanoscale phonon transport where the characteristic time and length are comparable with phonon relaxation time and mean free path, respectively, phonon transport is limited on both temporal and spatial scales. Also, different from the electron and optical wave packet emission, it is not easy to emit a perfect delta-function heat pulse in thermal experiments, which raises more problems in thermal experiments for detecting phonon superballistic transport. In this work, we report on the superballistic characteristics of ultrafast phonon transport both during and after the input of a heat pulse into a

[a)]Author to whom correspondence should be addressed: caoby@tsinghua.edu.cn. Tel./Fax: +86-10-6279-4531.

nanofilm, where phonon transport is in the ballistic-diffusive regime. They are described by a previously proposed model for electron wave packet spreading employing a point-source[8–10] and further explained by the superposition of heat pulses.

We first simulate the propagation of different types of heat pulses using the phonon Monte Carlo (MC) technique. The heat pulses employed and the phonon MC simulation system are illustrated in Fig. 1. Pulse 1 is a rectangular function with a heat flux density given as follows:

$$q = \begin{cases} \frac{1}{2} \times 5 \times 10^{11}, & t < t_p \\ 0, & t \geq t_p. \end{cases} \tag{2}$$

Here, $t_p = 2$ ps. The heat flux densities of pulse 2 and pulse 3 are given as follows:

$$q = \begin{cases} \frac{1}{2}\left(1 - \cos\left(\frac{2\pi}{t_p}t\right)\right) \times 5 \times 10^{11}, & t < t_p \\ 0, & t \geq t_p. \end{cases} \tag{3}$$

A sinusoidal function is a general selection that is often used in heat pulse propagation simulations and experiments.[28,35] Here, the periods of heat input are $t_p = 2$ ps and 0.2 ps for pulse 2 and pulse 3, respectively. Pulse 4 represents a pair of pulses based on pulse 3 emitted in succession. The four heat pulses are employed for the following specific purposes. Pulse 1 is simulated for studying superballistic phenomena during the process of heat pulse input into the nanoscale film ($0 < t < t_p$), while pulse 2 is simulated for investigating superballistic phenomena after the heat-input process is completed ($t > t_p$), i.e., during which the heat pulse propagates across the nanofilm. Finally, pulse 3 and pulse 4 are simulated to verify our theoretical analyses. The heat pulse propagation process in nanofilms is described by the phonon Boltzmann transport equation with relaxation time approximation, which is solved by a phonon-traced MC method[36–38] in this work. With the temperature results, the energy MSD-time relationships can be calculated by Eq. (1). We did not take into account the effects from the phonon spectrum and phonon dispersion but adopted the gray approximation (an even phonon frequency distribution is assumed) and Debye approximation for the phonon spectrum and dispersion relation in our phonon MC simulations. The phonon group velocity v_g is 5000 m/s, and the phonon relaxation time τ is 11.2 ps. The phonon mean free path is then calculated to be 56 nm. Since the heat pulse did not arrive at the reflection boundary in the simulations, the thickness of the nanofilm is not one of the key parameters. Greater details regarding the phonon MC simulation method and its settings can be obtained from previous studies.[28,36–38]

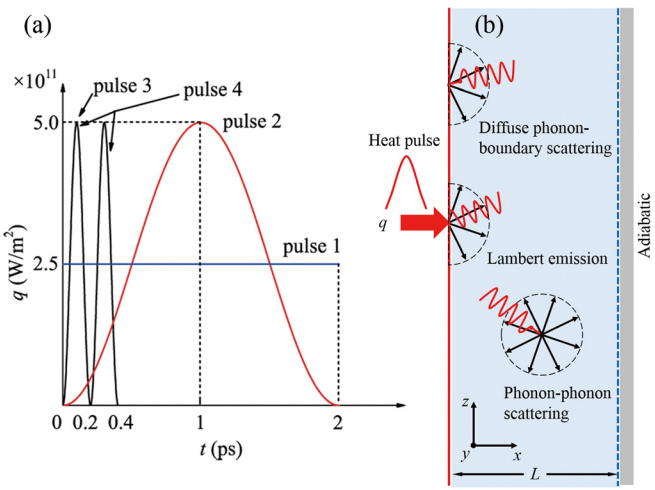

FIG. 1. (a) Heat pulses employed in the present study and (b) the simulation system, including phonon emission and phonon scattering.

The superballistic characteristics, present in transient phonon ballistic-diffusive transport, are introduced and analyzed in the heat pulse input process and heat pulse propagation process, respectively. In the following two paragraphs, we focus on the former process. Prior to discussion, it is necessary to first explain the method employed for calculating the energy MSD during the heat pulse input process. Since the total energy in the film increases during the input process, Eq. (1) cannot reflect the increase in the total energy, and the normalization procedure will affect the final results of β. Consequently, we redefine the energy MSD in the input process of heat pulse 1 as

$$\langle \sigma^2(t) \rangle = \int_0^X (E(x,t) - E_0)(x - x_0)^2 dx, \tag{4}$$

where the normalization procedure has been eliminated. The energy MSD in the input process can be well fitted by a power function of time with $\beta = 2.96$. Based on the above stated principles, $\beta > 2$ is characteristic of the superballistic phenomenon. Because the phonon relaxation time is much greater than the period of heat pulse input, phonon transport should be theoretically in an almost completely ballistic regime, which makes it unclear why superballistic characteristics are involved in this process.

To have a better understanding and description of the superballistic characteristics occurring during the process by which the heat pulse is input into the nanofilm, the point-source model,[8] originally proposed for analyzing the superballistic spreading of the electron wave packet, in particular, quantum systems,[8–10] is adopted for the photon transport phenomena discussed in this work because the two scenarios exhibit similar superballistic characteristics, e.g., a value of β that can be equal to 3. The previously proposed point-source model consists of a point source of electron wave packet emission

$$P(t) = \exp(-\Gamma t), \tag{5}$$

where Γ is a constant electron wave packet emission rate and a variance is given by

$$M_{PS}(t) = \int_0^\infty dx x^2 \int_0^t dt'(-\dot{P}(t'))\delta(x - v(t - t')), \tag{6}$$

where $-\dot{P}(t')$ is the flux emitted from the point source and v is the particle velocity. While $P(t) = \exp(-\Gamma t)$ can be approximated by the first-order term as $P(t) = 1 - \Gamma t$ when $t < 1/\Gamma$, the cubic term dominates the variance, which is approximated as

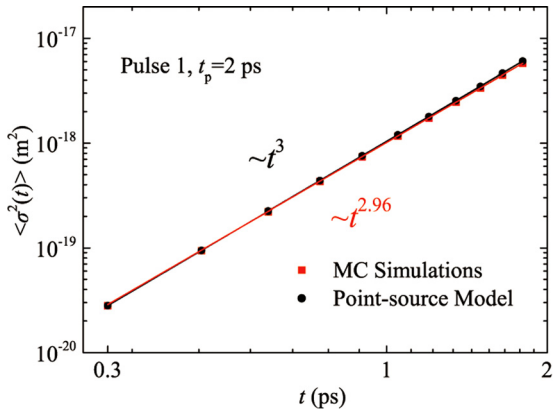

FIG. 2. Energy MSD-time relationships calculated from the simulation results of pulse 1 and the point-source model. Superballistic characteristics obtained during the process of the heat pulse input into the nanofilm are well modeled using the previously proposed point-source model.[8–10]

$$M_{PS}(t) = \frac{1}{3}v^2\Gamma t^3. \tag{7}$$

In brief, the model assumes that the effect of the localization of a disordered lattice can be treated as equal to a point source emitting electron wave packets, where the emission is a linear function of t in the early period, and the wave packets propagate in the ballistic regime in a perfect lattice. A value of $\beta = 3$ then results from a combination of the linear emission and quadratic ballistic propagation. The requirements of this model are well satisfied in the case of pulse 1 because pulse 1 is a rectangular pulse whose emission energy is a linear function of time, denoted as qt. In addition, phonon transport during the time interval of 0–2 ps is in an almost completely ballistic regime since the characteristic time is much less than the phonon relaxation time of 11.2 ps. The value of $\beta = 2.96 \approx 3$ from the MC simulations shown in Fig. 2 is consistent with that predicted by the point-source model, where we employed the values of $v = \sqrt{2}v_g/2$ (Ref. 28) and $\Gamma = q$. The results shown in Fig. 2 then confirm that the superballistic characteristics in the case of pulse 1 can be accurately modeled using the point-source model based on a simple physical construct.

The energy MSD-time relationships for pulse 2 calculated after the input of the heat pulse into the nanofilm, i.e., for $t > 2$ ps, based on Eq. (1) are shown in Fig. 3(a), with the corresponding values of β shown in Fig. 3(b). Superballistic characteristics are again present with $\beta > 2$ in the early period of heat pulse propagation. Because the time range of the heat pulse propagation process is much greater than that of the heat pulse input process, we can observe that β changes from a state reflecting superballistic characteristics to that reflecting ballistic-diffusive characteristics, i.e., from $\beta < 2$ to $\beta > 2$. While a value of β in the range of 1–2 can be well explained and understood from the perspective of phonon ballistic-diffusive transport, further discussion regarding the case of $\beta > 2$ is required. Actually, previous investigations related to MSD-time relationships have focused on delta-function heat pulse propagation.[3,4] However, a heat pulse cannot be effectively treated as a delta-function pulse when the heat pulse propagation time is not sufficiently large compared with the heat pulse period t_p. In the following discussion, we focus on the effect of a non-negligible value of t_p to find the reason why the observed transient phonon ballistic-diffusive transport includes superballistic characteristics.

The effect of a non-negligible value of the heat pulse period can also be called the superposition effect of the delta-function heat pulses since the heat pulse with a non-negligible period can be regarded as the superposition of infinite delta-function heat pulses. To show this effect clearly, we assume a process containing the propagation of two identical delta-function heat pulses, where one heat pulse is input into the nanofilm at $t = 0$ and the other is input at $t = t_0$. Then, we consider these two heat pulses collectively and calculate the overall energy MSD-time relationships at t ($t > t_0$). For the first heat pulse (with values indicated by subscripts 1), the energy MSD is given as

$$\langle\sigma_1^2(t)\rangle = \frac{\int_0^{X_1}(E_1(x,t)-E_{01})(x-x_{01})^2dx}{\int_0^{X_1}(E_1(x,t)-E_{01})dx} = 2D_1t^{\beta_1}. \tag{8}$$

Meanwhile, for the second pulse, this is given as

$$\langle\sigma_2^2(t)\rangle = \frac{\int_0^{X_2}(E_2(x,t)-E_{02})(x-x_{02})^2dx}{\int_0^{X_2}(E_2(x,t)-E_{02})dx} = 2D_2(t-t_0)^{\beta_2}. \tag{9}$$

D_1 and D_2 are the corresponding diffusive coefficients. Then, the energy MSD for both heat pulses collectively is given as

$$\langle\sigma^2(t)\rangle = \frac{\int_0^{\max(X_1,X_2)}(E(x,t)-E_0)(x-x_0)^2dx}{\int_0^{\max(X_1,X_2)}(E(x,t)-E_0)dx}, \tag{10}$$

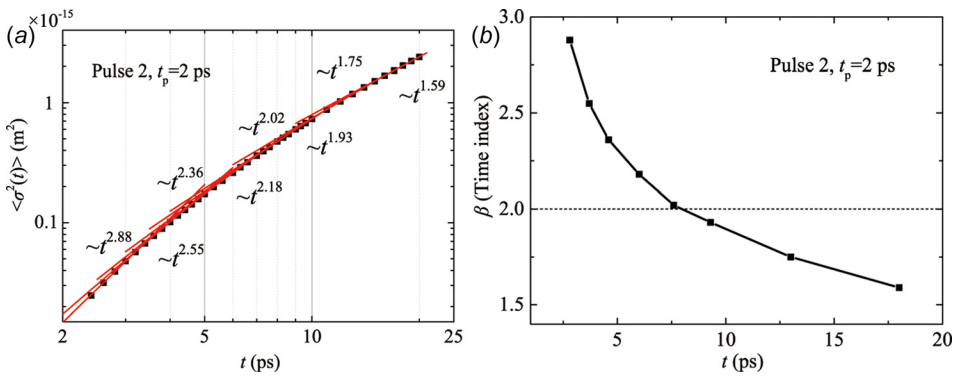

FIG. 3. Superballistic characteristics obtained after the process of inputting heat pulse 2 into the nanofilm: (a) Energy MSD-time relationships and (b) time index β.

which can be written as

$$\langle \sigma^2(t) \rangle = \frac{\int_0^{\max(X_1,X_2)} (E_1(x,t) - E_{01})(x - x_{01})^2 + (E_2(x,t) - E_{02})(x - x_{02})^2 dx}{\int_0^{\max(X_1,X_2)} (E_1(x,t) - E_{01}) + (E_2(x,t) - E_{02}) dx}. \quad (11)$$

Several simplifications must be explained here. Because phonon transport is described in this work by the linear Boltzmann transport equation with relaxation time approximation, the background energy does not influence the results. Thus, E_{01} and E_{02} are set to $E_{01} = E_{02} = 0$ for simplicity. The location where the heat pulse is input represents the zero point, i.e., $x_{01} = x_{02} = 0$. A larger spreading area and greater dissipation will be obtained for the first heat pulse because it propagates for a longer period, such that $X_1 > X_2$ and $\beta_1 < \beta_2$. The total energy of the two heat pulses in the nanofilm is equivalent once both have been completely input into the nanofilm at time t such that

$$\int_0^{X_1} (E_1(x,t) - E_{01}) dx = \int_0^{X_2} (E_2(x,t) - E_{02}) dx = \sum E. \quad (12)$$

Based on Eqs. (8)–(12), we can simplify the energy MSD of these two heat pulses collectively as

$$\langle \sigma^2(t) \rangle = \left(D_1 t^{\beta_1} + D_2 (t - t_0)^{\beta_2} \right) \sim t^{\beta}. \quad (13)$$

Under specific conditions, curve fitting to the energy MSD values given by Eq. (13) using a power function of time may yield $\beta > \beta_2$. As a result, a larger value of β may be obtained owing to the superposition of the delta-function heat pulses. For completely ballistic transport, $\beta_1 = \beta_2 = 2$ such that $\beta > 2$. To develop a deeper qualitative description of the superposition effect of heat pulses and the resulting level of superballistic characteristics, a dimensionless parameter denoted as the relative superposition time (RST) is defined as

$$\mathrm{RST} = t_s / t, \quad (14)$$

where t_s is the time of the superposition, which is given as t_0 in the case of the propagation of two delta-function heat pulses and t_p in the case of the propagation of a heat pulse with a non-negligible period. For heat pulses with a non-negligible period, RST is always less than 1 in the heat pulse propagation process and decreases during propagation. For a delta-function heat pulse, RST = 0. It is not difficult to show that, when RST approaches zero, β approaches β_2, and both approach β_1. The effect of the superposition of heat pulses will be observable when a heat pulse of the non-negligible period cannot be effectively treated as a delta-function heat pulse unless the propagation time is much greater than t_p. In other words, the effect of the superposition increases with increasing RST and vanishes when RST is close to or equal to zero. These analyses regarding the superposition effect are also applicable for explaining the superballistic characteristics observed during the heat pulse input process although a difference exists in that RST is always equal to 1, and the total energy in the nanofilm continuously increases during the input process, which maintains a large value of β. The above discussion clarifies why superballistic energy MSD-time relationships are obtained from the simulations of phonon ballistic-diffusive transport: the time index of the ballistic-diffusive transport ($\beta \leq 2$) increases due to the superposition effect and shows the superballistic characteristics ($\beta > 2$). Furthermore, to observe the superballistic characteristics in experiments of transient phonon transport, both the superposition effect and phonon ballistic-diffusive transport should be required, which means that both the RST and time Knudsen number ($\mathrm{Kn}_t = \tau/t$) should be large. Specifically, we present some cases where requirements can be satisfied as examples here. In time-domain thermoreflectance (TDTR) measurements, phonons in the metal transducer heated through electron-phonon scatterings may create a continuous phonon emission source for measured dielectric films. In ultrafast/nanoscale phonon transport across an interface, a continuous phonon emission source for the material on the other side may also be generated due to phonon localization at the interface. While phonon ballistic-diffusive transport is guaranteed by appropriate characteristic time, heat pulse conditions ensuring the superposition effect can be satisfied indirectly with these continuous phonon emission sources.

To verify our analyses regarding the superposition effect, simulations involving pulses 3 and 4 were conducted in which an ultra-short heat pulse with a period $t_p = 0.2$ ps was approximated as a delta-function heat pulse and succession

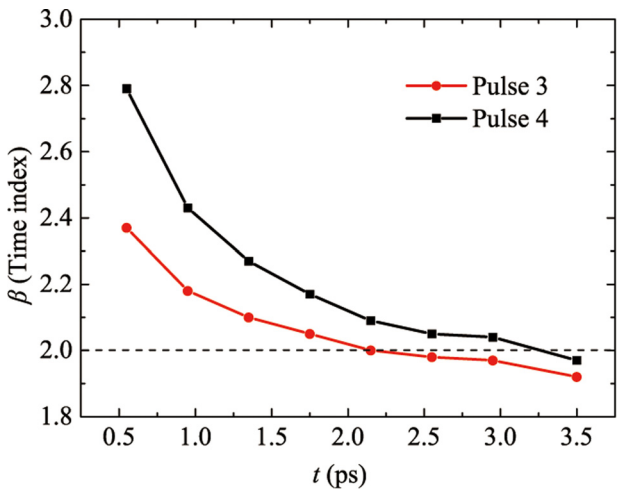

FIG. 4. Time index values obtained for pulse 3 and pulse 4. That the values of β increase due to the superposition of the two heat pulses of pulse 4 and that the difference between the two cases diminishes with decreasing RST verify the analysis presented.

emission of it was approximated as the superposition of the delta-function heat pulses. The corresponding simulation results are shown in Fig. 4. We note that the value of β in the case of pulse 4 is always greater than that in the case of pulse 3, showing the superposition effect of the heat pulses on the energy MSD-time relationships. The values of β eventually reduce to the interval representative of ballistic-diffusive transport, and the difference between the values of β for the cases of pulse 3 and pulse 4 diminishes with decreasing RST.

In the phonon MC simulations, we adopt the relaxation time approximation and gray approximation, without considering the influence of the phonon spectrum and realistic phonon scattering. However, it is reasonable to adopt the relaxation time approximation for silicon at room temperature.[39] The gray approximation is often used in theoretical investigations of phonon transport. The phonon spectrum will complicate the results and may play a crucial role, which will be studied in future work. Since the principle of the point source model is that an increase in the time index results from the combination of the propagation process and emitting process, it has nothing to do with the approximations adopted in our simulations, such as the gray approximation. Consequently, the principle can work for realistic physical systems. However, parameters in this model differ for different transport processes due to their dependence on the properties of physical systems, e.g., phonon spectrum. For this reason, further adjustment of parameters is necessary for realistic physical systems.

In conclusion, we have demonstrated that transient phonon ballistic-diffusive transport can include the superballistic characteristics, where the time indexes of the energy MSD-time relationships are greater than 2. Detailed analyses were conducted for these unique phenomena both during and after the process of heat pulse input into a nanofilm based on simulations of the propagation of different types of heat pulses using the phonon MC technique. The results demonstrated that the superballistic characteristics can be accurately modeled using a point-source model proposed for electron wave packet spreading and that these phenomena can be further explained by the superposition of heat pulses according to a dimensionless parameter RST. With a potential phenomenological description for the superballistic characteristics, this work will help to better understand relevant experiments and provide guidance for detecting the superballistic phonon transport.

This work was financially supported by the National Natural Science Foundation of China (Nos. 51676108 and 51356001), Science Fund for Creative Research Group (No. 51621062), and the Tsinghua National Laboratory for Information Science and Technology of China (TNList).

[1]M. C. Wang and G. E. Uhlenbeck, Rev. Mod. Phys. **17**, 323 (1945).
[2]K. R. Naqvi and S. Waldenstrom, Phys. Rev. Lett. **95**, 065901 (2005).
[3]B. W. Li and J. Wang, Phys. Rev. Lett. **91**, 044301 (2003).
[4]G. Zhang and B. W. Li, J. Chem. Phys. **123**, 014705 (2005).
[5]W. J. Yao and B. Y. Cao, Sci. Bull. **59**(27), 3495 (2014).
[6]G. Zimbardo, A. Greco, and P. Veltri, Phys. Plasmas **7**, 1071 (2000).
[7]Q. F. Zhao, C. A. Muller, and J. B. Gong, Phys. Rev. E **90**, 022921 (2014).
[8]L. Hufnagel, R. Ketzmerick, T. Kottos, and T. Geisel, Phys. Rev. E **64**, 012301 (2001).
[9]Z. J. Zhang, P. Q. Tong, J. B. Gong, and B. W. Li, Phys. Rev. Lett. **108**, 070603 (2012).
[10]B. P. Nguyen, Q. M. Ngo, and K. Kim, J. Korean Phys. Soc. **68**, 387 (2016).
[11]M. Sassetti, H. Schomerus, and U. Weiss, Phys. Rev. B **53**, R2914(R) (1996).
[12]J. Fourier, *Analytical Theory of Heat* (Dover Publications, New York, 1955).
[13]M. Mafdziaraz, A. Weron, K. Burnecki, and J. Klafter, Phys. Rev. Lett. **103**, 180602 (2009).
[14]A. Piryatinska, A. I. Saichev, and W. A. Woyczynski, Physica A **349**, 375 (2005).
[15]R. Metzler and J. Klafter, Phys. Rev. E **61**, 6308 (2000).
[16]K. Burnecki and A. Weron, Phys. Rev. E **82**, 021130 (2010).
[17]M. A. Desposito and A. D. Vinales, Phys. Rev. E **80**, 021111 (2009).
[18]Y. Meroz, M. Sokolov, and J. Klafter, Phys. Rev. Lett. **110**, 090601 (2013).
[19]M. Battiato, K. Carva, and P. M. Oppeneer, Phys. Rev. Lett. **105**, 027203 (2010).
[20]M. Battiato, K. Carva, and P. M. Oppeneer, Phys. Rev. B **86**, 024404 (2012).
[21]S. Redner, Physica D **38**, 287 (1989).
[22]J. A. Johnsom, A. A. Maznev, J. Cuffe, J. K. Eliason, A. J. Minnich, T. Kehoe, C. Torres, G. Chen, and K. Nelson, Phys. Rev. Lett. **110**, 025901 (2013).
[23]A. Majumdar, J. Heat Transfer **115**(1), 7 (1993).
[24]H. Y. Chiu, V. V. Deshpande, H. W. Ch. Postma, C. N. Lau, C. Miko, L. Forro, and M. Bockrath, Phys. Rev. Lett. **95**, 226101 (2005).
[25]M. Pumarol, M. Rosamond, P. Tovee, M. Petty, D. Zeze, V. Falko, and O. Kolosov, Nano Lett. **12**(6), 2906 (2012).
[26]A. Joshi and A. Majumdar, J. Appl. Phys. **74**, 31 (1993).
[27]Y. Ezzahri and A. Shakouri, Phys. Rev. B **79**, 184303 (2009).
[28]D. S. Tang, Y. C. Hua, B. D. Nie, and B. Y. Cao, J. Appl. Phys. **119**, 124301 (2016).
[29]S. Stutzer, T. Kottos, A. Tunnermann, S. Nolte, D. N. Christodoulides, and A. Szameit, Opt. Lett. **38**, 4675 (2013).
[30]R. Metzler and J. Klafter, Phys. Rep. **339**, 1 (2000).
[31]M. F. Shlesinger, J. Stat. Phys. **10**, 421 (1974).
[32]R. Kubo, Rep. Prog. Phys. **29**, 255 (1966).
[33]P. Siegle, I. Goychuk, and P. Hanggi, Phys. Rev. Lett. **105**, 100602 (2010).
[34]S. Iubini, O. Boada, Y. Omar, and F. Piazza, New J. Phys. **17**, 113030 (2015).
[35]H. D. Wang, W. G. Ma, X. Zhang, W. Wang, and Z. Y. Guo, Int. J. Heat Mass Transfer **54**, 967 (2011).
[36]J. M. Peraud and N. G. Hadjiconstantinou, Appl. Phys. Lett. **101**, 153114 (2012).
[37]Y. C. Hua and B. Y. Cao, Int. J. Heat Mass Transfer **78**, 755 (2014).
[38]Y. C. Hua and B. Y. Cao, Proc. R. Soc. A **472**, 20150811 (2016).
[39]A. Ward and D. A. Broido, Phys. Rev. B **81**, 085205 (2010).